© 2015. Published by The Company of Biologists Ltd | Journal of Experimental Biology (2015) 218, 3381-3390 doi:10.1242/jeb.125229

RESEARCH ARTICLE

Chemical cues from fish heighten visual sensitivity in larval crabs through changes in photoreceptor structure and function

Corie L. Charpentier* and Jonathan H. Cohen

ABSTRACT

Several predator avoidance strategies in zooplankton rely on the use of light to control vertical position in the water column. Although light is the primary cue for such photobehavior, predator chemical cues or kairomones increase swimming responses to light. We currently lack a mechanistic understanding for how zooplankton integrate visual and chemical cues to mediate phenotypic plasticity in defensive photobehavior. In marine systems, kairomones are thought to be amino sugar degradation products of fish body mucus. Here, we demonstrate that increasing concentrations of fish kairomones heightened sensitivity of light-mediated swimming behavior for two larval crab species (*Rhithropanopeus harrisii* and *Hemigrapsus sanguineus*). Consistent with these behavioral results, we report increased visual sensitivity at the retinal level in larval crab eyes directly following acute (1–3 h) kairomone exposure, as evidenced electrophysiologically from *V*–log *I* curves and morphologically from wider, shorter rhabdoms. The observed increases in visual sensitivity do not correspond with a decline in temporal resolution, because latency in electrophysiological responses actually increased after kairomone exposure. Collectively, these data suggest that phenotypic plasticity in larval crab photobehavior is achieved, at least in part, through rapid changes in photoreceptor structure and function.

KEY WORDS: Phenotypic plasticity, Zooplankton, Zoea, Vision, Kairomones, Photobehavior

INTRODUCTION

Many zooplankton exhibit phenotypically plastic defense strategies following detection of predator chemical cues. These chemical cues are defined as kairomones because they are interspecific signal molecules that benefit the receiver (Brönmark and Hansson, 2012). Predator kairomones have been shown to induce phenotypically plastic changes in defensive behavior of zooplankton. For instance, exposure to kairomones has been shown to alter photobehavior that is important to predator avoidance, including descent responses with rapid decreases in downwelling light (i.e. shadow responses; Cohen and Forward, 2003). Many zooplankton species also descend with small increases in downwelling light, and these responses are thought to contribute to depth regulation behavior, such as diel vertical migration (Cohen and Forward, 2009; Ringelberg, 2010; Williamson et al., 2011). Diel vertical migration is thought to be the greatest migration of biomass on Earth and generally describes a habitual night-time ascent to food-abundant surface waters and a daytime descent to darker waters (Hays, 2003). This daytime descent has long been proposed as a strategy to avoid visual predators (Stich and Lampert, 1981). More recent work supports diel vertical migration as a predator evasion strategy because kairomones increase swimming responses to light in marine and freshwater zooplankton (Cohen and Forward, 2005; Forward and Rittschof, 2000; Van Gool and Ringelberg, 2002). Kairomones affect defensive photobehavior after exposure times ranging from 5 min to several hours (Forward and Rittschof, 1993, 2000) and these changes are reversible after the removal of predator cues in several species (Bollens and Frost, 1989; Forward and Hettler, 1992).

Although light is the primary cue for this defensive photobehavior and kairomone exposure can increase such responses, other exogenous cues influence photobehavior and depth regulation in zooplankton, including temperature, salinity and food availability (Williamson et al., 2011). Temperature gradients or thermoclines often act as a barrier during depth regulation (Haney, 1993; Kessler, 2004; Cooke et al., 2008) and tidal cues, such as salinity, can influence vertical distribution and phototaxis in estuarine and coastal zooplankton species that regulate estuarine export or retention during different phases of their life history (Latz and Forward, 1977; Cronin and Forward, 1986; Welch and Forward, 2001). In addition, laboratory studies indicate that starvation affects phototaxis, such that animals activate an ascent response following decreases in downwelling light or maintain shallower daytime depths (Forward and Hettler, 1992; Haney, 1993). In marine systems, kairomones involved in defensive photobehavior are thought to be degradation products of external body mucus sloughed from fish and ctenophores and probably contain disaccharide glycosaminoglycans (Rittschof and Cohen, 2004).

Although previous work has demonstrated that zooplankton respond behaviorally to light stimuli at lower intensities in the presence of predator kairomones (Forward and Rittschof, 2000; Cohen and Forward, 2005), we currently lack a mechanism for these observed increases in photobehavioral responses, which are important for predator avoidance. Larval crabs offer a fitting model for better understanding kairomone-induced changes to defensive photobehavior because zoea larvae predictably maintain a depth near the isolume of their threshold for light detection (Forward, 1985; Sulkin, 1984) and kairomones exaggerate photobehavior important to predator evasion in larvae of at least one crab species, *Rhithropanopeus harrisii* (Cohen and Forward, 2003; Forward and Rittschof, 2000). The estuarine mud crab *R. harrisii* spends its entire life history within the estuary, including four planktonic zoeal stages (Cronin, 1982). However, most estuarine crab larvae migrate into coastal waters during their early planktonic stages. Since peak abundance of planktivorous estuarine fish coincides with seasonal crab spawning on the Atlantic coast of the United States (Hagan and Able, 2003; Forward, 2009; Epifanio, 2013), this migration is likely to decrease vulnerability to estuarine predators (Christy, 2011). Such an 'export-and-return' pattern of larval development and recruitment has been proposed for the rocky

School of Marine Science and Policy, College of Earth, Ocean and Environment, University of Delaware, 700 Pilottown Road, Lewes, DE 19958, USA.

*Author for correspondence (charpecl@udel.edu)

Received 13 May 2015; Accepted 30 August 2015

Journal of Experimental Biology (2015) 218, 3381-3390 doi:10.1242/jeb.125229

intertidal crab *Hemigrapsus sanguineus* (Cohen et al., 2015; Epifanio, 2013; Park et al., 2005). Thus, a comparison among crab species of kairomone-mediated changes to photosensitivity may yield differences related to predation pressures experienced during larval development.

The main objective of this study was to deduce whether kairomones affect photobehavior by increasing visual sensitivity at the retinal level in two larval crab species, *R. harrisii* and *H. sanguineus*. As previously described, light is thought to be the primary cue for defensive photobehavior in zooplankton with other factors, such as kairomones, modifying the behavioral response to light (Cohen and Forward, 2009). Hence, a probable mechanism for how kairomones affect photobehavior, which is important for predator avoidance via depth regulation, is by increasing visual sensitivity, whereby zooplankton exposed to kairomones exhibit behavioral and physiological responses to dimmer changes in light than they would otherwise. In a vertical migration scenario, for instance, this might place zooplankton at overall deeper depths in the water column throughout the diel cycle (Forward, 1985). Visual sensitivity may be controlled by structural and/or physiological mechanisms, as both play important roles mediating diel changes in visual sensitivity in crustaceans (Meyer-Rochow, 1999, 2001) and other arthropods (Battelle, 2002; Warrant et al., 2014). Here, electroretinogram (ERG) recordings and histological methods are employed to investigate kairomone-induced changes to retinal physiology and eye structure that could increase visual sensitivity and thereby result in kairomone-induced increases in photobehavior.

A second objective of this study was to compare defense photobehavior of decapod larvae that utilize two different early life history strategies: estuarine retention in *R. harrisii* and export-and-return in *H. sanguineus*. The presence or magnitude of predator kairomone-induced changes to photobehavior may vary between species that experience different levels of predation pressure during larval development, such as *R. harrisii* and *H. sanguineus*.

MATERIALS AND METHODS

Experimental solutions

Seawater used in all experiments was collected from Indian River Inlet [~32 practical salinity units (psu)], Delaware, USA. Biologically active molecules were removed by ultrafiltration (100 kDa; GE Life Sciences UFP-100-C-5A) and aging in darkness for at least 1 week (Forward and Rittschof, 1999). This water served as control seawater for rearing and all experiments. We produced kairomone solutions with diluted mucus, isolated from *Fundulus heteroclitus*. We isolated fish mucus with a previously described body wipe method (Forward and Rittschof, 1999) and diluted it with control seawater to produce uniform concentrations of 0.1, 0.01 or 0.001 g wet weight mucus l^{-1} seawater. Aliquots of concentrated mucus were stored at −80°C but were thawed and diluted immediately before using in experiments. Mucus from *F. heteroclitus* at similar concentrations has been shown to elicit strong behavioral responses in zooplankton (Forward and Rittschof, 1999, 2000; Cohen and Forward, 2005). However, it is unlikely that responses to kairomones are specific to predator species, because similar behavioral effects have been observed in animals exposed to kairomones from multiple fish and gelatinous invertebrate species (McKelvey and Forward, 1995).

Crab collection and rearing

During summer (May–September) of 2013, we collected ovigerous female crabs from either Broadkill River, DE, USA [*Rhithropanopeus harrisii* (Gould 1841)] or Roosevelt Inlet, DE, USA [*Hemigrapsus sanguineus* (De Haan 1853)]. We maintained females in the laboratory under a 14 h:10 h light:dark cycle at ~23°C in control seawater (20 psu for *R. harrisii* and 30 psu for *H. sanguineus*). On the day of hatching, larvae from single female broods were placed into fresh control seawater and water changes were conducted three times per week. We fed larvae newly hatched brine shrimp (*Artemia franciscana*) nauplii *ad libitum*.

Behavioral experiments

We conducted behavioral experiments in an apparatus that mimics the underwater angular light distribution, similar to that used by Forward et al. (1984). Within a light-tight enclosure, we placed groups of zoeae (N≈30) in a transparent acrylic chamber (5×5×5 cm), enclosed within a larger black acrylic water bath (40×40×15 cm; ~23°C). Experimental light was produced by an Oriel 300 W Xe Arc Lamp (Newport, Irvine, CA, USA), and filtered to 488 nm with an interference filter (10 FWHM, Melles Griot 03FIL002, Irvine, CA, USA). We chose this wavelength, because it is near peak spectral sensitivity in *R. harrisii* and *H. sanguineus* (Cohen et al., 2015; Forward and Costlow, 1974). Fixed neutral density filters (Melles Griot, Irvine, CA, USA) allowed us to control the intensity of light stimuli, which passed horizontally through a collimating lens, electromagnetic shutter (Newport), wavelength and intensity filters and then reflected off a mirror inside the light-tight enclosure to pass vertically through a white acrylic diffuser that covered the water bath. The described light assembly produces a relatively diffuse downwelling light source, entering a dark larval chamber. Prior to experiments, we measured downwelling irradiance at the larval chamber with an optometer and calibrated radiometric probe (models S471 and 247; Gamma Scientific, Baltimore, MD, USA) to select an appropriate range and resolution of light stimuli.

We recorded swimming behavior through two narrow transparent sections in the black water bath with a digital camera (scA750-60gm; Basler AG Electronics, Ahrensburg, Germany) with a 16 mm varifocal lens (HF16HA-1B; Fujinon Corp, Edison, NJ, USA), backlit by an infrared LED array (880 nm; Advanced Illumination, Edmund Optics, Barrington, NJ, USA). Camera optics were set such that the field of view and depth of field could resolve all swimming individuals within the chamber, regardless of their position in the three-dimensional chamber. We used a custom program in LabVIEW (National Instruments, Austin, TX, USA) to coordinate timing of shutter opening and closing as well as capture video recordings.

Behavioral experiments were conducted on stage 4 *R. harrisii* and stage 3 *H. sanguineus* zoeae, because larvae at these stages are active swimmers that exhibit strong phototactic responses (Forward and Rittschof, 2000; Cohen et al., 2015). In addition, exposure to fish kairomones resulted in enhanced photoresponses in stage 4 *R. harrisii* zoeae from the Neuse River estuary, North Carolina, USA (Forward and Rittschof, 2000). We conducted similar behavioral experiments in this study, because no such evidence exists for either larval *H. sanguineus* or *R. harrisii* populations in Delaware Bay, USA. Prior to behavioral experiments, animals were exposed to either control seawater or kairomone solutions of three concentrations (0.1, 0.01 and 0.001 g mucus l^{-1} seawater) for 1–3 h and acclimated to the dark for at least 1 h, 15 min of which were in the experimental chamber. After the acclimation period, experimental animals experienced a series of six 3 s light stimuli increasing in intensity from approximately 5×10^{11} to 5×10^{13} photons m^{-2} s^{-1} in *R. harrisii* and 1×10^{11} to 1×10^{13} photons m^{-2} s^{-1} in *H. sanguineus*. During these experiments, 4 min of dark acclimation time separated each stimulus. We recorded swimming behavior 3 s before ('dark') and after each light stimulus. Behavioral experiments were replicated five times for both species, and each replicate represents a brood from a single mother to account for potential maternal effects.

We determined start and end X- and Y-coordinates of swimming individuals in each 3 s video recording using a PC-based motion analysis system (CellTrak software, Motion Analysis, Santa Rosa, CA, USA). An individual was considered to be descending if the line between its start and end coordinates were within nadir ±60 deg. We then calculated the percentage descending for each group (replicate×treatment) before (dark) and after each light stimulus. Within each treatment, we compared percentage descending in the dark with percentage descending after each of the given light stimuli with one-way repeated measures (RM) ANOVAs. If RM ANOVAs detected significant differences (P<0.05), Holm–Šidák *post hoc* tests determined which specific light stimuli evoked a significant descent response relative to swimming behavior in the dark. The light stimulus of the lowest intensity that induced a descent response was deemed

Journal of Experimental Biology

Journal of Experimental Biology (2015) 218, 3381-3390 doi:10.1242/jeb.125229

the 'behavioral threshold'. One-way ANOVAs within treatments suggested that percentage of descending animals swimming in the dark did not differ significantly between replicates (P>0.05). Hence, we used mean percentage descending before each light stimulus as 'percentage descending in the dark' in the RM ANOVA analyses described above. All statistical analyses were conducted in SigmaPlot 12.0 (Systat Software, San Jose, CA).

Electrophysiology

We measured extracellular electroretinograms (ERGs) on stage 4 *R. harrisii* and stage 3 *H. sanguineus* zoeae. Prior to experiments, animals were exposed to either control seawater or kairomones at 0.1 g mucus l^{-1} seawater for at least 1 h. This kairomone concentration was chosen because it induced strong behavioral responses in both species (Fig. 1). In ERG experiments, zoeae were attached by their dorsal carapace to the plastic head of a pin with cyanoacrylate gel adhesive (Loctite, Rocky Hill, CT, USA) and then suspended in a 19°C water bath of their respective treatment by a plexiglass support. We then placed the recording electrode, a tungsten microelectrode (127 µm tip, A-M Systems, Sequim, WA, USA), subcorneally in the eye and a second differential electrode with the same specifications in the water bath. Differential AC signals were amplified (Ext-02 B, NPI Electronic Instruments, Germany), digitized and stored in LabChart 7 (AD Instruments) for analysis of peak-to-peak response height and response time.

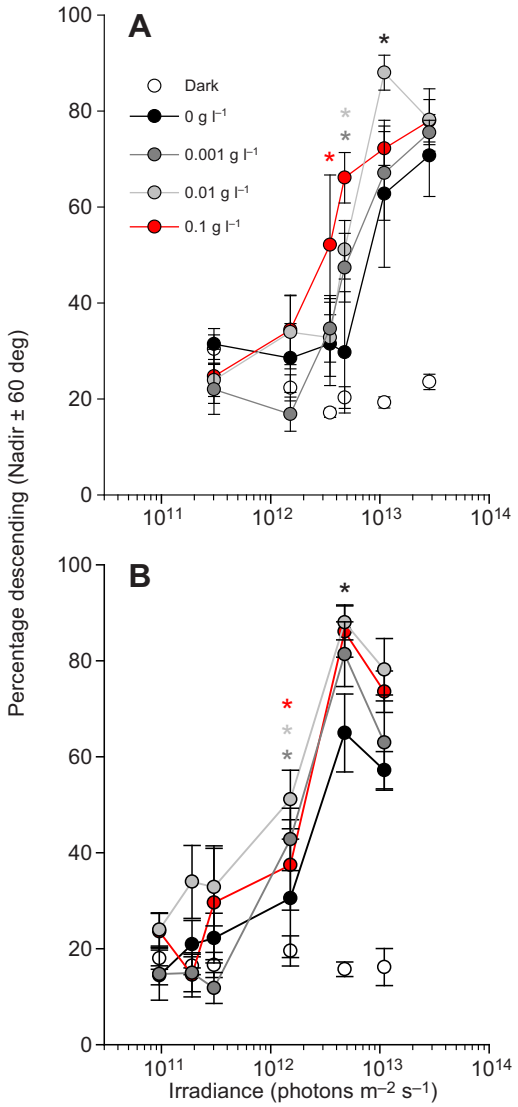

Fig. 1. Behavioral thresholds of photobehavior in *Rhithropanopeus harrisii* and *Hemigrapsus sanguineus* larvae. Mean±s.e.m. percentage descending (±60 deg) of (A) stage 4 *R. harrisii* and (B) stage 3 *H. sanguineus* zoeae before (swimming in the dark) and after light stimulation. Animals (~30 individuals) in each replicate (N=5) were exposed to either control seawater (0 g l^{-1}) or kairomones from *Fundulus heteroclitus* mucus at 0.1, 0.01 or 0.001 g mucus l^{-1} seawater. Behavioral thresholds, or significant differences in percentage descending before and after light stimulation, were determined by one-way repeated measures ANOVAs with Holm–Šidák *post hoc* tests and accepted at P<0.05. These thresholds are represented by asterisks of respective treatment symbol colors. Data shown here for animals swimming in the dark are the combined means±s.e.m. of all four treatments.

Light stimuli were produced by a quartz halogen lamp (DC-150, Dolan-Jenner Industries, Boxborough, MA, USA) and delivered to the eye with a 4-mm-diameter liquid light guide. Wavelength was set by a blue/green broadband pass filter (BG-18, Schott, Elmsford, NY, USA) and light intensity controlled with fixed neutral density filters (Melles Griot, Irvine, CA, USA). Again, we chose this wavelength, because it is near peak spectral sensitivity for *R. harrisii* and *H. sanguineus* (Cohen et al., 2015; Forward, 2009). An electromagnetic shutter and shutter driver (LS6S2T0-100, VCM-D1, Uniblitz/Vincent Associates, Rochester, NY, USA) under computer-controlled stimulus onset and duration. Sensitivity may differ between night and day in crustaceans (Meyer-Rochow, 1999, 2001), so we conducted all experiments during the day between 09:00 h and 16:00 h. Prior to experiments, irradiance was measured with a spectroradiometer (USB4000; Ocean Optics, Dunedin, FL, USA) to determine the range and resolution of light stimuli.

Response-intensity (V–log I) curves were generated from ERG recordings, where response magnitude (peak-to-peak height) increased with intensity until reaching some maximum response (V_{max}). We acclimated animals in the dark prior to experiments and did not give an experimental flash until the ERG response to a dim test flash consistently yielded a consistent response magnitude. Experimental flashes (100 ms) were given in order of increasing irradiance, ranging from 10^{11}–10^{16} photons m^{-2} s^{-1}. Between experimental flashes, animals acclimated in the dark for at least 2 min, but total acclimation time was determined with intermittent test flashes during experiments.

To generate V–log I curves, we plotted peak-to-peak response height across the intensity range of given light stimuli. We normalized individual curves to V_{max} and modeled the response–intensity relationship with the Zettler modification of the Naka–Rushton equation to determine the curve's half saturation point (log K), V_{max}, slope and dynamic range or log range from 5 to 95% of V_{max} (Frank, 2003). Here, log K was defined as a measure of physiological sensitivity. As such, lower values indicate greater sensitivity. In this analysis, we only included curves that had a measured V_{max} value at least 80% of the model's estimated V_{max}. We assessed differences in log K, slope, and dynamic range with t-tests, comparing individuals exposed to control seawater (N=5) and kairomones (N=5) in *R. harrisii* and *H. sanguineus*. We conducted statistical analyses in SigmaPlot 12.0, and differences were considered significant if P<0.05. As in behavioral experiments, replicates were taken from a brood from a single mother to avoid possible maternal effects.

In addition, we investigated the kinetics of ERG responses at each irradiance for the generated V–log I curves (N=5 for each treatment), specifically the time from the light stimulus onset to the response start (response latency) and to the response peak (peak latency). Response start was defined as the point at which the ERG signal begins to decrease in magnitude above background noise. We assessed the effect of treatment and irradiance on response and peak latency with two-way ANOVAs. Again, we conducted all statistical analyses in SigmaPlot 12.0, and accepted significant differences at P<0.05.

Histology: eye structure

We applied histological techniques to observe possible kairomone-induced changes in eye structure that could increase visual sensitivity over a 3 h time interval. We exposed stage 4 *R. harrisii* and stage 3 *H. sanguineus* zoeae to kairomones from 0.1 g mucus l^{-1} seawater for a period of 0 (control seawater), 0.5, 1 or 3 h (N=10 at each time interval). Following exposure, we removed and fixed heads in 2.5% glutaraldehyde in 0.4 mol l^{-1} Millonig's buffer solution for 3.25 h between 08:00 h and 13:00 h under fluorescent

Journal of Experimental Biology (2015) 218, 3381-3390 doi:10.1242/jeb.125229

room light (~10^{18} photons m^{-2} s^{-1} white light). Larvae were dehydrated in a graded ethanol series, gradually transferred into medium grade acrylic resin (London White Company, London, UK) and embedded in resin by hot curing at 60±2°C for 20–24 h in an Isotemp oven (Fisher Scientific, Waltham, MA, USA). We then cut semi-thin (0.2 µm) sections with a Sorvall MT-2B Ultramicrotome (Du Pont, Tucson, AZ, USA) and stained these sections with a mixture of Toludine Blue O and Basic Fuchsin (Electron Microscopy Sciences, Hatfield, PA, USA) before mounting on slides.

From the slides, we measured several characteristics of eye structure with an ocular reticle on a compound microscope (CX31, Olympus, Tokyo, Japan). These included rhabdom diameter, rhabdom length, aperture diameter and length of crystalline cone (see below). Here, we measured rhabdom diameter at the distal end of the rhabdom and estimated aperture diameter as the distance between distal accessory pigments surrounding the crystalline cone. All measurements were from longitudinally sectioned ommatidia in the anterior/dorsal quadrant of the eye, and measurements were only used if all the above-mentioned characteristics were present. To ensure that the structural characteristics did not vary with ommatidia location, we divided the anterior/dorsal quadrant of the eye into three portions: anterior, intermediate and lateral. These were 0–25 deg, 25–65 deg, and 65–90 deg from the anteriormost ommatidium, respectively, ranging dorsally from the frontal to the sagittal plane. Since the chosen characteristics of eye structure did not vary between these three locations in control animals (one-way ANOVA), all measurements taken from the anterior/dorsal quandrant of the eye were used in analysis. In addition, structural parameters were measured blindly, i.e. treatment was not identified until after all measurements were completed. We calculated the grand mean of all measurements taken from an individual zoea and this grand mean was considered a replicate. Since we only used measurements from ommatidia that contained all structural characteristics, the number of replicates decreased slightly from N=10 to N=8, 6, 5 and 7 in *R. harrisii* and N=6, 6, 4 and 6 in *H. sanguineus* exposed to kairomones for 0 (control), 0.5, 1 or 3 h, respectively. We took digital images of each measured section with a digital camera (EOS Rebel T3i, Canon, Japan), and qualitatively compared distribution of screening pigments.

Optical sensitivity of larval crab compound eyes, S (µm^2 Sr) was calculated according to Land (1981; Eqn 1). We calculated optical sensitivity to compare control and kairomone-treated animals and to determine whether changes in eye structure resulted in optical sensitivity differences:

$$S = \left(\frac{\pi}{4}\right)^2 A^2 \left(\frac{d}{f}\right)^2 \left(\frac{kl}{2.3 + kl}\right). \quad (1)$$

Structural characteristics in the sensitivity equation include aperture diameter (A), rhabdom diameter (d), focal length (f), the absorption coefficient (k) and rhabdom length (l). Since focal length of an apposition compound eye is typically the distance from the nodal point of the corneal lens to the distal tip of the rhabdom, we estimated focal length to be the length of the crystalline cone. This estimation began at the distal tip of the crystalline cone rather than the nodal point of the corneal lens, because the corneal lens was separated from its corresponding crystalline cone in some sections. Further, the thickness of the corneal lens was approximately 2–3 µm in both *R. harrisii* and *H. sanguineus*, and the nodal point within would be less than this total distance. Since the crystalline cone extends from just beneath the corneal lens to the distal tip of the rhabdom in all sections, with length ranging from 23 to 30 µm, ignoring the distance between the nodal point of the corneal lens and the distal tip of the crystalline cone in our estimation of focal length should introduce little error. We used an absorption coefficient of 0.008 µm^{-1} (Cronin and Forward, 1988).

We also calculated acceptance angle using several structural characteristics (Eqn 2; Snyder, 1979), including facet diameter (D), rhabdom diameter (d), and focal length (f):

$$\Delta\rho = \sqrt{\left(\frac{\lambda}{D}\right)^2 + \left(\frac{d}{f}\right)^2}. \quad (2)$$

Facet diameter (D) was measured after initial analysis of eye structure, but these diameters were consistent between control and kairomone-treated animals; mean values of 20 and 19 µm were used for *R. harrisii* and *H. sanguineus*, respectively. Again, focal length was estimated to be the length of the crystalline cone. A wavelength (λ) of 500 nm was used to represent peak spectral sensitivity in *R. harrisii* and *H. sanguineus* (Cohen et al., 2015; Forward and Costlow, 1974).

To assess whether kairomone exposure affected eye structure, optical sensitivity and/or acceptance angle, we conducted a one-way ANOVA for each parameter, comparing animals exposed to kairomones for 0 (control), 0.5, 1 and 3 h. We then used a Holm–Šidák *post hoc* test to make multiple comparisons of all kairomone treatments (0.5, 1, 3 h) versus the control. Values of optical sensitivity and acceptance angle were log transformed for analysis. We conducted all statistical analyses in SigmaPlot 12.0, and accepted significant differences at P<0.05. All individuals used in experiments came from a single female in both *R. harrisii* and *H. sanguineus*.

Estimated changes to depth

We compared downwelling irradiance with depth at two times of day with the behavioral thresholds in *R. harrisii* with and without kairomone exposure in order to assess the magnitude of depth change expected with kairomone exposure. At a site in Delaware Bay where larval *R. harrisii* are abundant (38°57.862′ N, 75°16.093′ W), we measured spectral irradiance just below the surface to a depth of 3.25 m at midday in August 2014 (Hydro-Rad-3, HOBI Labs, Bellevue, WA, USA). Spectral irradiance at each depth interval was weighted by the spectral sensitivity of *R. harrisii* larvae determined electrophysiologically (Forward et al., 2014) and then integrated to yield light intensity as 'crab-utilized photons'. These integrated values were used to determine a diffuse attenuation coefficient (K_d) of 1.4 m^{-1} by linear regression and used in the Lambert–Beer equation as a simplified model of light attenuation with depth (e.g. Gallegos, 2001) to determine irradiance (crab-utilized photons) over the water column. A similar irradiance profile was modeled for twilight using the same K_d value, but assuming irradiance just below the surface to be two orders of magnitude less than that at midday, based on previous observations (Cohen and Forward, 2005). With these two depth profiles of irradiance as crab-utilized photons, we calculated the expected change in depth of *R. harrisii* based on our observed behavioral thresholds from behavioral experiments with and without kairomone exposure.

RESULTS

Defensive photobehavior

We conducted behavioral experiments in an apparatus that mimics the underwater angular light distribution, characterized by a relatively bright, diffuse light from above entering a dark chamber. In experiments, we exposed crab larvae to an intensity range of downwelling light stimuli and measured their swimming responses. The behavioral threshold was quantified and used as a proxy for defensive photobehavior; this threshold was defined here as the lowest light intensity to evoke a descent swimming response in a group of larvae when compared with swimming direction of pre-stimulus behavior in darkness. We exposed larvae to control seawater or kairomones from fish mucus at three concentrations (0.1, 0.01, 0.001 g mucus l^{-1} seawater) for 1–3 h before they were used in experiments. The percentage of larvae descending while swimming in darkness between successive light stimuli did not differ throughout each experiment, and mean percentage of animals descending in the dark ranged from 19–24% in *R. harrisii* and 10–22% in *H. sanguineus*. In both species, percentage descending differed before and after light stimulation in all treatments (P<0.001; one-way repeated-measures ANOVAs).

Kairomone exposure decreased behavioral thresholds for light-evoked descents (Fig. 1; Table 1). In stage 4 *R. harrisii* zoeae, the behavioral threshold was 1.10×10^{13} photons m^{-2} s^{-1} in animals

Journal of Experimental Biology (2015) 218, 3381-3390 doi:10.1242/jeb.125229

Table 1. Behavioral threshold, physiological sensitivity and optical sensitivity in *R. harrisii* and *H. sanguineus* exposed to control seawater or seawater with kairomones

		Behavioral threshold (log photons m^{-2} s^{-1})	Physiological sensitivity (log photons m^{-2} s^{-1})	Optical sensitivity (μm^2 Sr)
Rhithropanopeus harrisii	Control	13.0	14.37±0.57	0.009±0.003
	Kairomones	12.5*	13.53±0.10	0.034±0.009*
Hemigrapsus sanguineus	Control	12.7	14.23±0.22	0.015±0.006
	Kairomones	12.2*	13.50±0.21*	0.022±0.007

Behavioral thresholds (log photons m^{-2} s^{-1}) were determined in analysis of photobehavior experiments (Fig. 1). Physiological sensitivity (means±s.e.) was defined as the log *K* value (log photons m^{-2} s^{-1}) of *V*–log *I* curves (Fig. 2; *n*=5); lower values indicate greater sensitivity. Optical sensitivity (μm^2 Sr) was calculated from structural characteristics using the Land equation (Eqn 1) and values shown (means±s.e.) are from animals that were exposed to kairomones from *Fundulus heteroclitus* mucus (0.1 g l^{-1}) for 0 h (control; *N*=8, 6) or 1 h (kairomones; *N*=6, 4) in *R. harrisii* and *H. sanguineus*, respectively. Significant differences (*P*<0.05) are represented by an asterisk and were determined using repeated-measures ANOVAs with Holm–Šidák *post hoc* tests for behavioral thresholds, *t*-tests for physiological sensitivity and one-way ANOVAs with Holm–Šidák *post hoc* tests for optical sensitivity.

exposed to control seawater. Relative to the control, animals exposed to the two lowest kairomone concentrations (0.01 and 0.001 g mucus l^{-1} seawater) had behavioral thresholds that were half that of the control at 4.77×10^{12} photons m^{-2} s^{-1} and thresholds in animals exposed to the highest kairomone concentration (0.1 g mucus l^{-1} seawater) were a third of the control threshold at 3.48×10^{12} photons m^{-2} s^{-1} (Fig. 1A).

In stage 3 *H. sanguineus* zoeae, the behavioral threshold was 4.77×10^{12} photons m^{-2} s^{-1} in the control. Thresholds decreased to about a third of the control at 1.51×10^{12} photons m^{-2} s^{-1} after exposure to kairomones at all three concentrations (Fig. 1B). The behavioral threshold shift in kairomone-exposed animals was similar in *R. harrisii* and *H. sanguineus*. However, behavioral thresholds were lower in *H. sanguineus* overall, i.e. *H. sanguineus* in the control had a behavioral threshold that was half that of *R. harrisii*.

Electrophysiology

We generated response–intensity (*V*–log *I*) curves from extracellular electroretinograms (ERGs) to investigate whether kairomones alter retinal physiology to increase visual sensitivity and therefore influence changes to photobehavior observed in previous experiments. Prior to electrophysiological experiments, animals were exposed to either control seawater or kairomones at 0.1 g mucus l^{-1} seawater for 1–3 h. Kairomone exposure resulted in a shift of *V*–log *I* curves to lower intensities in both *R. harrisii* and *H. sanguineus* (Fig. 2), consistent with increased visual sensitivity. Furthermore, physiological sensitivity was defined here as the half-saturation (log *K*) of *V*–log *I* curves and log *K* values were lower in kairomone-exposed than in control animals, also suggesting increased visual sensitivity (Fig. 2; Table 1). However, this difference was only significant in *H. sanguineus* (*P*=0.04; *t*-test). In addition, we observed decreases in V_{max} following kairomone exposure (Table 2), with significant differences between control and kairomone treatments in *H. sanguineus*. No significant differences were detected in the slope or dynamic range of *V*–log *I* curves (Table 2).

We also assessed temporal resolution by measuring latency of the ERG response relative to the stimulus flash at each irradiance of *V*–log *I* curves. Specifically, we compared the time from light stimulus onset to response start (response latency) and to response maximum (peak latency) between control and kairomone-treated animals. In addition, the response start was defined as the point at which the ERG signal begins to decrease in magnitude above background noise. Response waveform varied between control and kairomone treatments, and response tended to be of smaller magnitude and reach the response maximum more quickly in kairomone-exposed animals than in the control (Fig. 2). In *R. harrisii*, response and peak latency decreased with increasing irradiance (*P*<0.009) and after kairomone exposure (*P*<0.001; Fig. 3A,B; two-

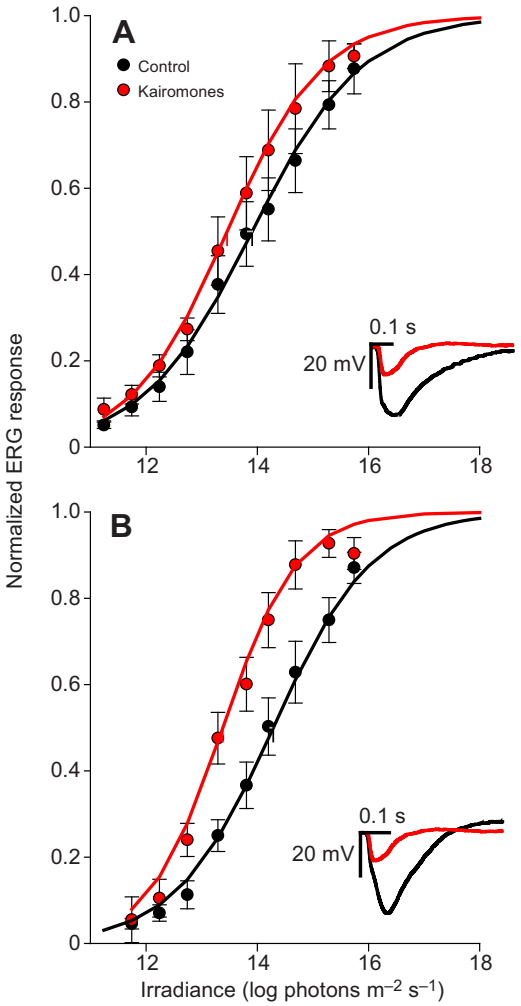

Fig. 2. Response–intensity curves for *R. harrisii* and *H. sanguineus* larvae. Mean±s.e.m. normalized ERG responses across a log range of irradiances (photons m^{-2} s^{-1}), in (A) stage 4 *R. harrisii* and (B) stage 3 *H. sanguineus* zoeae exposed to control seawater (*N*=5) or kairomones from *Fundulus heteroclitus* mucus at 0.1 g mucus l^{-1} seawater (*N*=5). Curves were modeled using the Zettler modification of the Naka–Rushton equation and log *K* of each curve is indicated by a dotted line of its respective treatment color. Insets with each *V*–log *I* curve are representative ERG response waveforms at log *K* of control and kairomone-treated animals, with length of light stimulus (0.1 s) and response magnitude indicated by scale bars. The timescale of insets is positioned at the onset of the light stimulus.

Journal of Experimental Biology (2015) 218, 3381-3390 doi:10.1242/jeb.125229

Table 2. Response–intensity curve parameters in *R. harrisii* and *H. sanguineus* exposed to control seawater or seawater with kairomones

		V_{max} (mV)	Slope	Dynamic range (log photons m^{-2} s^{-1})
Rhithropanopeus harrisii	Control	1.41±0.37	0.48±0.02	5.41±0.26
	Kairomones	0.47±0.47	0.53±0.07	4.69±0.34
Hemigrapsus sanguineus	Control	0.80±0.16	0.59±0.04	4.27±0.37
	Kairomones	0.36±0.06*	0.70±0.07	3.89±0.55

Values (means±s.e.m.) of V_{max}, slope, and dynamic range were derived from the Zettler modification of the Naka–Rushton model (N=5). Significant differences between control and kairomone treatments were accepted at P<0.05 (t-test) and represented by an asterisk.

way ANOVAs). In *H. sanguineus*, response latency decreased with increasing irradiance (P<0.001; Fig. 3C) and peak latency was shorter after kairomone exposure (P<0.001; Fig. 3D). The interaction between treatment and irradiance was not significant in either species.

Eye structure

Using light microscopy of semi-thin sections, we compared several characteristics of eye structure (Fig. 4A) in control and kairomone-exposed zoeae. Rhabdom diameter was measured at the distal tip of the rhabdom and aperture diameter was defined as the distance between distal accessory pigments at the base of the crystalline cone in longitudinal sections. Prior to fixation and embedding, animals were exposed to kairomones at a concentration of 0.1 g mucus l^{-1} seawater for durations of 0 (control), 0.5, 1 or 3 h. Kairomone-induced changes to photobehavior in crustacean larvae are evoked over this timeframe (Forward and Rittschof, 1993, 2000). In *R. harrisii*, rhabdom diameter and length differed between kairomone-exposed and control animals (P=0.04 and 0.03, respectively; one-way ANOVA). Specifically, rhabdom diameter was significantly wider in *R. harrisii* exposed to kairomones for 1 and 3 h, relative to control animals (Fig. 4B). In addition, rhabdom length was shorter in *R. harrisii* exposed to kairomones for 3 h, compared with the control (Fig. 4D). In *H. sanguineus*, rhabdom diameter also differed after kairomone exposure (P=0.05; one-way ANOVA). Rhabdoms widened after 3 h of kairomone exposure relative to control animals (Fig. 4C). However, differences in rhabdom length were not statistically significant between the kairomone treatment and control in *H. sanguineus* (Fig. 4D). Cone length and aperture diameter did not vary across the 3 h kairomone exposure time in either species, and we did not observe changes in screening pigment quantity or position. In addition, we used characteristics of eye structure to calculate optical sensitivity (Eqn 1; Land, 1981) and acceptance angle (Eqn 2; Snyder, 1979). Mean optical sensitivity and acceptance angle increased after 1 h of kairomone exposure in both species (Tables 1 and 3). However, differences between the control and kairomone treatments were only significant in *R. harrisii* (P=0.03; one-way ANOVAs). Specifically, optical sensitivity increased after 1 h of kairomone exposure (Table 1) and acceptance angle was larger in animals exposed to kairomones for 0.5–3 h, relative to the control (Table 3).

DISCUSSION

In both *R. harrisii* and *H. sanguineus*, we observed changes to photobehavior that could impact predator-avoidance behavior, specifically decreases in the behavioral threshold following kairomone exposure (Fig. 1; Table 1). These results were comparable to findings with a North Carolina (USA) population of *R. harrisii* (Forward and Rittschof, 2000) and once established for our Delaware (USA) *R. harrisii* study population and now *H. sanguineus*, we investigated whether kairomones mediate these behavioral changes by increasing visual sensitivity. Visual sensitivity can be regulated with physiological and/or structural

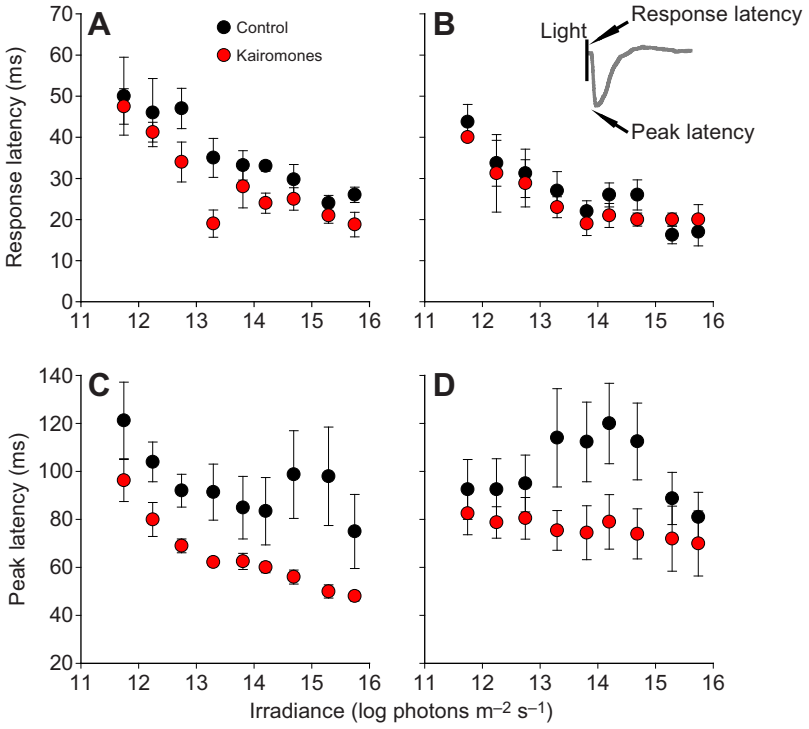

Fig. 3. Latency in ERG responses for *R. harrisii* and *H. sanguineus* larvae. Mean±s.e.m. response latency (ms) in (A) stage 4 *R. harrisii* and (B) stage 3 *H. sanguineus* zoeae as well as mean±s.e.m. peak latency (ms) in the same stage *R. harrisii* (C) and *H. sanguineus* (D) across a log range of irradiances (photons m^{-2} s^{-1}). Animals were exposed to either control seawater (N=5) or kairomones from *Fundulus heteroclitus* mucus at 0.1 g mucus l^{-1} seawater (N=5). As indicated by the inset, response latency was defined as the time from the light stimulus onset to the response start and peak latency as the time from the light stimulus onset to the response peak.

Journal of Experimental Biology

Journal of Experimental Biology (2015) 218, 3381-3390 doi:10.1242/jeb.125229

Table 3. Acceptance angle calculated from eye structure across kairomone exposure time in *R. harrisii* and *H. sanguineus*

Kairomone exposure time (h)	*Rhithropanopeus harrisii*		*Hemigrapsus sanguineus*	
	Δρ	*N*	Δρ	*N*
0	6.2±0.5	6	7.2±0.8	6
0.5	9.3±1.4*	6	6.8±0.6	6
1	9.3±0.9*	5	7.8±0.7	4
3	8.4±0.7*	7	8.1±0.6	6

Data are calculated values (means±s.e.m.) of acceptance angle (Δρ, deg) and sample size (*N*). Method for angle calculation is given in Eqn 2. Significant differences between control (0 h) and kairomone treatments (0.5, 1, 3 h) were accepted at $P<0.05$ by one-way ANOVAs with Holm–Šidák *post hoc* tests and represented by an asterisk.

mechanisms, e.g. changes to photoreceptor membrane potential and size (Meyer-Rochow, 2001).

Extracellular recordings in the retina suggest greater visual sensitivity in zoeae exposed to fish kairomones (Fig. 2; Table 1). Similar ERG methods have been used to assess light/dark adaptation and cyclic diel changes to sensitivity in crustaceans, where sensitivity increases during night-time hours (Aréchiga and Rodriguez-Sosa, 1998; Hariyama et al., 2001; Meyer-Rochow and Tiang, 1984; Yang et al., 1986), as well as at night in adult *H. sanguineus* with intracellular photoreceptor recordings (Arikawa et al., 1987). The observed pattern of increase in sensitivity of crab larvae following kairomone exposure matched these light/dark and diel changes in sensitivity of adult crustaceans, although were smaller in magnitude by about 25% (Hariyama et al., 2001). Hence, larval crabs exposed to kairomones may use similar physiological mechanisms at the retinal level to mediate phenotypic plasticity in defensive photobehavior, e.g. descent to darker waters during daytime when fish are abundant. Further work using intracellular recording could be used to determine the effect of kairomones on individual photoreceptors, as has been done to demonstrate higher night-time signal-to-noise ratios in photoreceptor cells of *Limulus* (Kaplan and Barlow, 1980).

Increases in visual sensitivity often come at the cost of temporal resolution (Warrant, 1999, 2008; Warrant et al., 2014). For example, higher sensitivity is associated with decreases in temporal resolution in mesopelagic and deep-sea crustaceans (Frank, 1999, 2000; Frank et al., 2012), and log *K* values are often negatively correlated with response latency in these animals (Frank, 2003). Here, we tested whether increases in visual sensitivity of kairomone-exposed animals resulted in a loss of temporal resolution by measuring latency in response onset and peak. Surprisingly, we found no indication of longer latency times in kairomone-exposed animals with heightened photoreceptor sensitivity; latency actually decreased after kairomone exposure (Fig. 3). Hence, kairomones do not increase sensitivity at the cost of temporal resolution in these larval crabs. Moreover, observed decreases in response amplitude and V_{max} after kairomone exposure (Fig. 2; Table 2) may allow for increases in visual sensitivity in conjunction with greater temporal resolution.

We also found changes to eye structure in kairomone-exposed animals. Rhabdoms were wider and shorter after 1–3 h of kairomone exposure in *R. harrisii* and were wider after 3 h of exposure in *H. sanguineus* (Fig. 4). This change in rhabdom diameter probably drove the observed increases in optical sensitivity in *R. harrisii* exposed to kairomones for 1 h, relative to those in the control (Table 1), although similar increases were not found in *H. sanguineus*. We would expect sensitivity changes to occur over this timeframe as crustacean larvae show behavioral responses to kairomones within 1 h, as demonstrated here and elsewhere (e.g. Forward and Rittschof, 1993; McKelvey and Forward, 1995). Chamberlain and Barlow (1987) similarly observed wider, shorter rhabdoms in *Limulus* at night when animals are known to be most visually sensitive. Furthermore, rhabdom size increased in adult *H. sanguineus* and several other adult crab species during the nocturnal phase of the diel cycle (Nässel and Waterman, 1979; Stowe, 1980; Toh and Waterman, 1982; Arikawa et al., 1987) and several studies have similarly reported greater rhabdom width or volume in more-sensitive dark-adapted eyes (Meyer-Rochow and

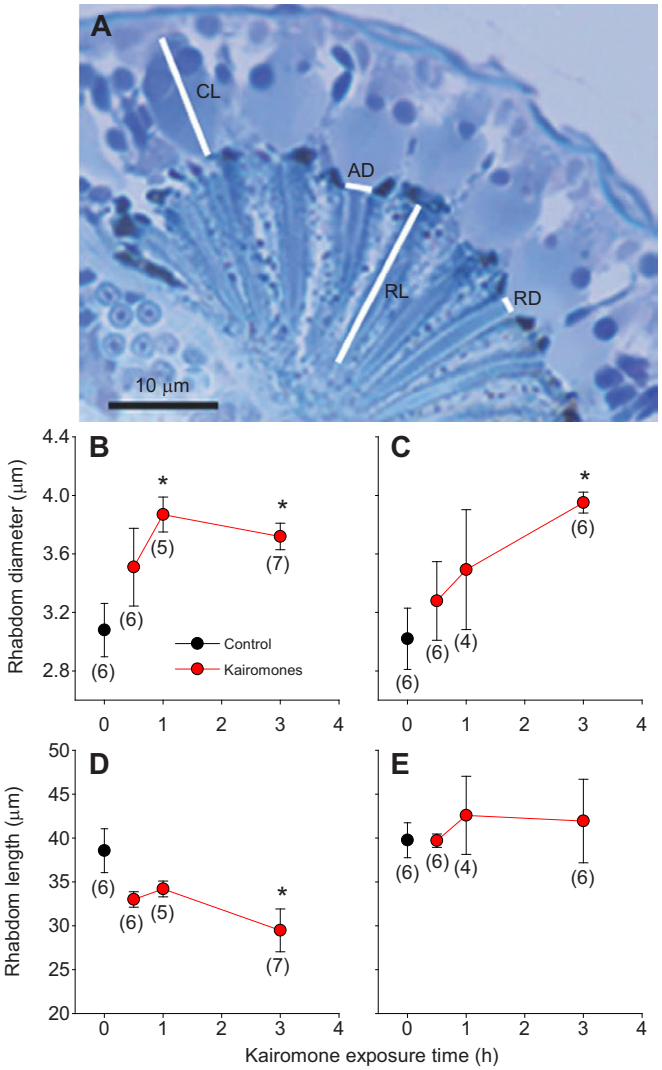

Fig. 4. Characteristics of eye structure in *R. harrisii* and *H. sanguineus* larvae. (A) Semi-thin (0.2 µm) longitudinal section from a stage 4 *Rhithropanopeus harrisii* zoeae compound eye. Structural characteristics used in analysis are highlighted in white and include cone length (CL), aperture diameter (AD), rhabdom length (RL), and rhabdom diameter at the distal tip (RD). Mean±s.e.m. rhabdom diameter (µm) in (B) stage 4 *Rhithropanopeus harrisii* and (C) stage 3 *Hemigrapsus sanguineus* zoeae, as well as mean± s.e.m. rhabdom length (µm) in the same stage (D) *R. harrisii* and (E) *H. sanguineus*. Zoeae were exposed to kairomones from *Fundulus heteroclitus* mucus at a concentration of 0.1 g l^{-1} for 0 (control), 0.5, 1 or 3 h, and sample size at each exposure time is shown in parentheses. Significant differences in rhabdom size between control and kairomone-exposed animals (0.5, 1, 3 h) were determined by one-way ANOVAs with Holm–Šidák *post hoc* tests, accepted if $P<0.05$, and represented by asterisks.

Journal of Experimental Biology

Journal of Experimental Biology (2015) 218, 3381-3390 doi:10.1242/jeb.125229

Tiang, 1984) or at night in other crustaceans (Hariyama et al., 2001; Matsuda and Wilder, 2014; Yuan et al., 1997).

Spatial summation is common in animals that need to resolve fast-moving objects as well as improve sensitivity (Warrant, 1999). Some crustaceans demonstrate spatial summation by increasing their visual acceptance angle (Bryceson and McIntyre, 1983; Hariyama et al., 2001) and other arthropod groups neurally pool information by laterally spreading and coupling the interneurons responsible for photoreceptor analysis (Greiner et al., 2004, 2005; Warrant et al., 2014). Here, we used characteristics of eye structure to determine visual acceptance angle. Since acceptance angle did increase after 0.5, 1 and 3 h of kairomone exposure in *R. harrisii* (Table 3), observed increases in sensitivity may be achieved through spatial summation. Hence, heightened sensitivity following kairomone exposure may be at the expense of spatial resolution, but zoeae maintain the ability to detect fast-moving objects such as predatory fish.

In this study, we observed kairomone-induced changes to rhabdom shape that may increase visual sensitivity. However, several structural characteristics, not observed here, also mediate sensitivity changes in compound eyes. For instance, although we did not find evidence of any screening pigment migration within ommatidia from either control or kairomone-treated animals, distribution of screening pigments often mediates a change in visual sensitivity, e.g. those seen over the diel cycle (Meyer-Rochow, 2001). In dark-adapted eyes or during the nocturnal phase of the diel cycle, screening pigments frequently migrate distally from the rhabdom or become more dispersed in crustacean compound eyes, including adult *H. sanguineus* (Arikawa et al., 1987; Cellier et al., 1998; Hariyama et al., 2001; Meyer-Rochow and Tiang, 1984). Although less commonly observed, Nilsson and Odselius (1981) found changes to the dioptric apparatus, including cone shortening and lens elongation, in dark-adapted, night-time eyes of *Artemia*. The authors concluded that these changes, along with additional differences in rhabdom shape, might increase sensitivity while maintaining spatial resolution by decreasing focal length and widening the area that can be used for light capture. However, we did not observe a similar result in crystalline cones of crab larvae.

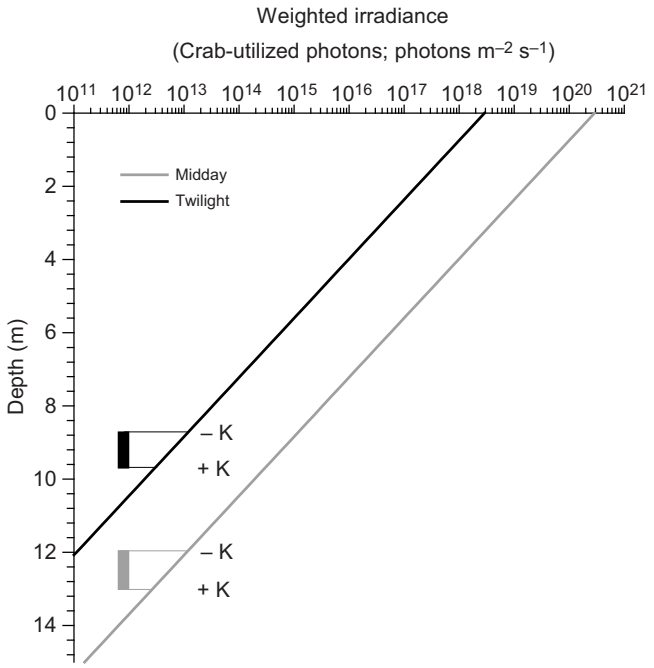

Fig. 5. Estuarine water column depth at the larval crab behavioral threshold. Solid lines are downwelling irradiance weighted by the spectral sensitivity of *R. harrisii* larvae, thereby representing the light utilized by the larval crab eye at a given depth (crab-utilized photons). Light at depth is calculated from surface irradiance of 2.9×10^{20} photons m^{-2} s^{-1} (midday) and 2.9×10^{18} photons m^{-2} s^{-1} (twilight), using a diffuse attenuation coefficient (K_d) of 1.4 m^{-1}. For each time of day, the depth difference for *R. harrisii* behavioral threshold with (+ K) and without kairomones (– K) is shown as an inset thickened vertical line, with horizontal lines indicating the light level at these behavioral thresholds.

We observed several physiological and structural differences in the retina that could lead to increased visual sensitivity, including higher physiological sensitivity, i.e. lower log *K* values in *H. sanguineus* and changes to rhabdom shape and optical sensitivity, which were most distinct in *R. harrisii*. However, some differences were too small to detect a kairomone effect, such as physiological sensitivity in *R. harrisii*, suggesting that factors other than increases in sensitivity directly at the retinal level may be involved in the observed shift in behavioral thresholds. Neural amplification or changes to photochemical processes could be contributing to the observed kairomone-induced changes to defensive photobehavior. Neural summation strategies, temporal or spatial, are often used to increase visual sensitivity. This is done by neurally increasing gain, e.g. summing input from neighboring visual channels (Warrant, 1999). Specific neural inputs that mediate sensitivity changes are rarely reported. However, intracellular electrophysiological recordings in *Limulus* suggest that efferent input from the optic nerve plays an important role in increasing response gain in photoreceptor cells and that octopamine probably acts as the neurotransmitter for these optic nerve pulses (Barlow et al., 1987; Battelle, 2002; Kaplan and Barlow, 1980). Alternatively, Blest and Stowe (1997) found that inhibition of phospholipase, an enzyme that is important for phototransduction, prevented the diurnal decreases in rhabdom diameter that occur during the diel cycle of an adult crab. This finding suggests potential photochemical control of rhabdom size. However, phospholipase enzymes are important to processes aside from phototransduction and changes to other biological pathways could be contributing to this result. Oberwinkler and Stavenga (2000) used calcium imaging to examine intracellular calcium levels in the rhabdomeres of blowflies and found that reduced sensitivity caused by light adaptation resulted in a decrease in the duration of calcium transients in the rhabdomere. In the case of increases in larval crab sensitivity upon kairomone exposure, similar mechanisms warrant investigation.

In addition to investigating the mechanism by which kairomones increase defensive photobehavior, we also aimed to identify potential differences in the phenotypic plasticity of behavior and visual sensitivity between two crab species with different early life history strategies: estuarine retention (*R. harrisii*) and offshore transport (*H. sanguineus*). More drastic increases in photobehavior might be expected in *R. harrisii*, because these crabs spend their entire life history within the estuary (Forward, 2009) and probably experience higher predation pressure than *H. sanguineus*, which is exported offshore during larval development before returning to the coast (Christy, 2011; Epifanio, 2013; Hagan and Able, 2003). Conversely, the kairomone effect on behavior was similar in *R. harrisii* and *H. sanguineus* after exposure to the highest mucus concentration, and behavioral thresholds were lower in *H. sanguineus* than in *R. harrisii* overall, regardless of kairomone exposure or

concentration (Fig. 1). Furthermore, a larger kairomone effect in *R. harrisii* was not clearly demonstrated in our electrophysiological and histological investigation of visual sensitivity. In fact, *V*–log *I* curves suggest a greater kairomone-induced sensitivity increase in *H. sanguineus* (Fig. 2; Table 1), whereas changes to eye structure that would increase visual sensitivity, namely rhabdom shape, were more distinct in *R. harrisii* (Fig. 4; Table 1). Overall, the observed physiological and structural changes are likely to play a similar role in mediating kairomone-induced increases in photobehavior in both species.

Here, we present evidence that kairomones affect photobehavior, specifically by lowering the behavioral threshold. Given that crab larvae maintain depth near the isolume of their threshold for light detection (Forward, 1985; Sulkin, 1984), we estimated how the observed physiological and behavioral changes after kairomone exposure would influence depth selection in the estuarine water column by modeling downwelling irradiance with depth at two times of day at a site in Delaware Bay where larval *R. harrisii* are abundant. Depth change in *R. harrisii* was estimated with and without kairomone exposure from the behavioral thresholds determined in behavioral experiments. With kairomone exposure, *R. harrisii* would reside approximately 1 m deeper than animals without kairomone exposure at both midday and twilight (Fig. 5). Assuming that kairomone production is positively related to predator abundance (Shephard, 1994; Van Gool and Ringelberg, 2002), such a descent to deeper, darker waters could limit feeding ability in visual predators. Indeed, Grecay and Targett (1996) demonstrated light-limited feeding in a common zooplanktivorous predator from this habitat – the juvenile weakfish *Cynoscion regalis*.

Conclusion

Behavioral strategies for predator avoidance are phenotypically plastic in several zooplankton species, where predator kairomones induce increases in swimming responses to light (Cohen and Forward, 2009; Ringelberg, 2010; Williamson et al., 2011). Here, we extend previously observed kairomone-induced changes to defensive photobehavior to another crab species and more importantly, report evidence that increases in visual sensitivity at the physiological and structural level in the eyes of both crab species are consistent with these behavioral changes. The kairomone effect on the observed behavioral and physiological responses was similar in the estuarine-retained *R. harrisii* and the offshore-transported *H. sanguineus*. Latency in electrophysiological responses decreased after kairomone exposure. Hence, it is unlikely that visual sensitivity increased at the expense of temporal resolution, although we present some evidence for spatial summation. In addition, we estimated changes in zooplankton depth with the observed decreases in the behavioral threshold of larval *R. harrisii* exposed to kairomones, and our model suggests that depth of these larval crabs would increase about 1 m with kairomone exposure. Overall, this study offers a potential mechanism to explain previous observations of phenotypic plasticity in photobehavior important to predator avoidance and vertical migrations in zooplankton.

Acknowledgements

We thank Alexander Wright, Cynthia Hanson, Margaret Blake and Heather Cronin for their assistance in crab collections and rearing. We also thank Dr David Kirchman for his insightful comments on an earlier draft of the manuscript.

Competing interests

The authors declare no competing or financial interests.

Author contributions

C.L.C. and J.H.C. developed the concept and approach, C.L.C. performed the experiments and data analysis, C.L.C. and J.H.C. prepared and revised the manuscript.

Funding

This work was supported in part by awards from the University of Delaware Research Foundation (award no. 12A00755) and Delaware Sea Grant (award no. NA10OAR4170084) to J.H.C.; Marian R. Okie and Joanne Currier Daiber fellowships to C.L.C.

References

Aréchiga, H. and Rodriguez-Sosa, L. (1998). Circadian clock function in isolated eyestalk tissue of crayfish. *Proc. R. Soc. Lond. B. Biol. Sci.* **265**, 1819-1823.
Arikawa, K., Kawamata, K., Suzuki, T. and Eguchi, E. (1987). Daily changes of structure, function and rhodopsin content in the compound eye of the crab *Hemigrapsus sanguineus*. *J. Comp. Physiol. A.* **161**, 161-174.
Barlow, R. B., Kaplan, E., Renninger, G. H. and Saito, T. (1987). Circadian rhythms in *Limulus* photoreceptors. I. Intracellular studies. *J. Gen. Physiol.* **89**, 353-378.
Battelle, B.-A. (2002). Circadian efferent input to *Limulus* eyes: anatomy, circuitry, and impact. *Microsc. Res. Techniq.* **58**, 345-355.
Blest, A. D. and Stowe, S. (1997). A phospholipase inhibitor, manoalide, and a G-protein activator, Mas-7, both affect the turnover of phototransductive membranes by crab retinas in darkness. *J. Comp. Physiol. A.* **810**, 347-355.
Bollens, S. M. and Frost, B. W. (1989). Zooplanktivorous fish and variable diel vertical migration in the marine planktonic copepod *Calanus pacificus*. *Limnol. Oceanogr.* **34**, 1072-1083.
Brönmark, C. and Hansson, L.-A. (2012). Chemical ecology in aquatic systems-an introduction. In *Chemical Ecology in Aquatic Systems* (ed. C. Brönmark and L.-A. Hansson), pp. 1-19. New York: Oxford University Press.
Bryceson, K. P. and McIntyre, P. (1983). Image quality and acceptance angle in a reflecting superposition. *J. Comp. Physiol. A.* **151**, 367-380.
Cellier, S., Rehaïlia, M., Berthon, J.-L. and Buisson, B. (1998). The role of the eye in the migratory rhythms of *Daphnia magna* and *Daphnia longispina* (Cladocera). *Annls. Limnol.* **34**, 159-164.
Chamberlain, S. C. and Barlow, R. B. (1987). Control of structural rhythms in the lateral eye of *Limulus*: interactions of natural lighting and circadian efferent activity. *J. Neurosci.* **7**, 2135-2144.
Christy, J. H. (2011). Timing of hatching and release of larvae by brachyuran crabs: patterns, adaptive significance and control. *Integr. Comp. Biol.* **51**, 62-72.
Cohen, J. H. and Forward, R. B. (2003). Ctenophore kairomones and modified aminosugar disaccharides alter the shadow response in a larval crab. *J. Plankton Res.* **25**, 203-214.
Cohen, J. H. and Forward, R. B., Jr. (2005). Photobehavior as an inducible defense in the marine copepod *Calanopia americana*. *Limnol. Oceanogr.* **50**, 1269-1277.
Cohen, J. H. and Forward, R. B., Jr. (2009). Zooplankton diel vertical migration - a review of proximate control. *Oceanogr. Mar. Biol.* **47**, 77-110.
Cohen, J. H., Hanson, C. K., Dittel, A. I., Miller, D. C. and Tilburg, C. E. (2015). The ontogeny of larval swimming behavior in the crab *Hemigrapsus sanguineus*: implications for larval transport. *J. Exp. Mar. Biol. Ecol.* **462**, 20-28.
Cooke, S. L., Williamson, C. E., Leech, D. M., Boeing, W. J. and Torres, L. (2008). Effects of temperature and ultraviolet radiation on diel vertical migration of freshwater crustacean zooplankton. *Can. J. Fish. Aquat. Sci.* **65**, 1144-1152.
Cronin, T. W. (1982). Estuarine retention of larvae of the crab *Rhithropanopeus harrisii*. *Estuar. Coast. Shelf S.* **15**, 207-220.
Cronin, T. W. and Forward, R. B. (1986). Vertical migration cycles of crab larvae and their role in larval dispersal. *Bull. Mar. Sci.* **39**, 192-201.
Cronin, T. W. and Forward, R. B. (1988). The visual pigments of crabs. I. Spectral characteristics. *J. Comp. Physiol. A* **162**, 463-478.
Epifanio, C. E. (2013). Invasion biology of the Asian shore crab *Hemigrapsus sanguineus*: a review. *J. Exp. Mar. Biol. Ecol.* **441**, 33-49.
Forward, R. B. (1985). Behavioral responses of larvae of the crab *Rhithropanopeus harrisii* (Brachyura: Xanthidae) during diel vertical migration. *Mar. Biol.* **90**, 9-18.
Forward, R. B., Jr. (2009). Larval biology of the crab *Rhithropanopeus harrisii* (Gould): a synthesis. *Biol. Bull.* **216**, 243-256.
Forward, R. B. and Costlow, J. D. (1974). The ontogeny of phototaxis by larvae of the crab *Rhithropanopeus harrisii*. *Mar. Biol.* **26**, 27-33.
Forward, R. B. and Hettler, W. F. (1992). Effects of feeding and predator exposure on photoresponses during diel vertical migration of brine shrimp larvae. *Limnol. Oceanogr.* **37**, 1261-1270.
Forward, R. B. and Rittschof, D. (1993). Activation of photoresponses of brine shrimp nauplii involved in diel vertical migration by chemical cues from fish. *J. Plankton. Res.* **15**, 693-701.
Forward, R. B. and Rittschof, D. (1999). Brine shrimp larval photoresponses involved in diel vertical migration: activation by fish mucus and modified amino sugars. *Limnol. Oceanogr.* **44**, 1904-1916.

Forward, R. B. and Rittschof, D. (2000). Alteration of photoresponses involved in diel vertical migration of a crab larva by fish mucus and degradation products of mucopolysaccharides. *J. Exp. Mar. Biol. Ecol.* **245**, 277-292.
Forward, R. B., Cronin, T. W. and Stearns, D. E. (1984). Control of diel vertical migration: photoresponses of a larval crustacean. *Limnol. Oceanogr.* **29**, 146-154.
Forward, R. B., Moeller, B. P. and Cohen, J. H. (2014). Circadian rhythm in larval release by the crab *Rhithropanopeus harrisii*: entrainment model. *Biol. Bull.* **226**, 92-101.
Frank, T. M. (1999). Comparative study of temporal resolution in the visual systems of mesopelagic crustaceans. *Biol. Bull.* **196**, 137-144.
Frank, T. M. (2000). Temporal resolution in mesopelagic crustaceans. *Philos. Trans. R. Soc.* **355**, 1195-1198.
Frank, T. M. (2003). Effects of light adaptation on the temporal resolution of deep-sea crustaceans. *Integr. Comp. Biol.* **43**, 559-570.
Frank, T. M., Johnsen, S. and Cronin, T. W. (2012). Light and vision in the deep-sea benthos: II. Vision in deep-sea crustaceans. *J. Exp. Biol.* **215**, 3344-3353.
Gallegos, C. L. (2001). Calculating optical water quality targets to restore and protect submersed aquatic vegetation: overcoming problems in partitioning the diffuse attenuation coefficient for photosynthetically active radiation. *Estuaries* **24**, 381-397.
Grecay, P. A. and Targett, T. E. (1996). Effects of turbidity, light level and prey concentration on feeding of juvenile weakfish *Cynoscion regalis*. *Mar. Ecol. Prog. Ser.* **131**, 11-16.
Greiner, B., Ribi, W. A., Wcislo, W. T. and Warrant, E. J. (2004). Neural organisation in the first optic ganglion of the nocturnal bee *Megalopta genalis*. *Cell Tissue Res.* **318**, 429-437.
Greiner, B., Ribi, W. A. and Warrant, E. J. (2005). A neural network to improve dim-light vision? Dendritic fields of first-order interneurons in the nocturnal bee *Megalopta genalis*. *Cell Tissue Res.* **322**, 313-320.
Hagan, S. M. and Able, K. W. (2003). Seasonal changes of the pelagic fish assemblage in a temperate estuary. *Estuar. Coast. Shelf Sci.* **56**, 15-29.
Haney, J. F. (1993). Environmental control of diel vertical migration behavior. *Arch. Hydrobiol. Beih. Ergebn. Limnol.* **39**, 1-17.
Hariyama, T., Meyer-rochow, V. B., Kawauchi, T., Takaku, Y. and Tsukahara, Y. (2001). Diurnal changes in retinula cell sensitivities and receptive fields (two-dimensional angular sensitivity functions) in the apposition eyes of *Ligia exotica* (Crustacea, Isopoda). *J. Exp. Biol.* **248**, 239-248.
Hays, G. C. (2003). A review of the adaptive significance and ecosystem consequences of zooplankton diel vertical migrations. *Hydrobiology* **503**, 163-170.
Kaplan, E. and Barlow, R. B. (1980). Circadian clock in *Limulus* brain increases response and decreases noise of retinal photoreceptors. *Nature* **286**, 393-395.
Kessler, K. (2004). Distribution of *Daphnia* in a trade-off between food and temperature: individual habitat choice and time allocation. *Freshwater Biol.* **49**, 1220-1229.
Land, M. F. (1981). Optics and vision in invertebrates. In *Handbook of Sensory Physiology*, Vol. VII/6B (ed. H. Autrum), pp. 471-592. Berlin: Springer.
Latz, M. I. and Forward, R. B. (1977). The effect of salinity upon phototaxis and geotaxis in a larval crustacean. *Biol. Bull.* **153**, 163-179.
Matsuda, K. and Wilder, M. N. (2014). Eye structure and function in the giant freshwater prawn *Macrobrachium rosenbergii*. *Fish. Sci.* **80**, 531-541.
Mckelvey, L. M. and Forward, R. B. (1995). Activation of brine shrimp nauplii photoresponses involved in diel vertical migration by chemical cues from visual and non-visual planktivores. *J. Plankton Res.* **17**, 2191-2206.
Meyer-Rochow, V. B. (1999). Compound eye: circadian rhythmicity, illumination, and obscurity. In *Atlas of Arthropod Sensory Receptors* (ed. E. Eguchi and Y. Tominaga), pp. 97-124. New York: Springer.
Meyer-Rochow, V. B. (2001). The crustacean eye: dark/light adaptation, polarization sensitivity, flicker fusion frequency, and photoreceptor damage. *Zool. Sci.* **18**, 1175-1197.
Meyer-Rochow, V. B. and Tiang, K. M. (1984). The eye of *Jasus edwardsii* (Crustacea, Decapoda): electrophysiology, histology, and behaviour. *Zoologica* **45**, 1-61.
Nässel, D. R. and Waterman, T. H. (1979). Massive diurnally modulated photoreceptor membrane turnover in crab light and dark adaptation. *J. Comp. Physiol. A.* **131**, 205-216.
Nilsson, D.-E. and Odselius, R. (1981). A new mechanism for light-dark adaptation in the *Artemia* compound eye (Anostraca, Crustacea). *J. Comp. Physiol. A.* **143**, 389-399.
Oberwinkler, J. and Stavenga, D. G. (2000). Calcium transients in the rhabdomeres of dark- and light-adapted fly photoreceptor cells. *J. Neurosci.* **20**, 1701-1709.
Park, S., Epifanio, C. E. and Iglay, R. B. (2005). Patterns of larval release by the Asian shore crab *Hemigrapsus sanguineus* (De Haan): periodicity at diel and tidal frequencies. *J. Shellfish Res.* **24**, 591-595.
Ringelberg, J. (2010). *Diel Vertical Migration of Zooplankton in Lakes and Oceans*. Dordrecht: Springer.
Rittschof, D. and Cohen, J. H. (2004). Crustacean peptide and peptide-like pheromones and kairomones. *Peptides* **25**, 1503-1516.
Shephard, K. L. (1994). Functions for fish mucus. *Rev. Fish Biol. and Fisher.* **4**, 401-429.
Snyder, A. W. (1979). Physics of vision in compound eyes. In *Handbook of Sensory Physiology*, Vol. VII/6A (ed. H. Autrum), pp. 225-313. Berlin: Springer.
Stich, H.-B. and Lampert, W. (1981). Predator evasion as an explanation of diurnal vertical migration by zooplankton. *Nature* **293**, 396-398.
Stowe, S. (1980). Rapid synthesis of photoreceptor membrane and assembly of new microvilli in a crab at dusk. *Cell Tissue Res.* **211**, 419-440.
Sulkin, S. D. (1984). Behavioral basis of depth regulation in the larvae of brachyuran crabs. *Mar. Ecol. Progr. Ser.* **15**, 181-205.
Toh, Y. and Waterman, T. H. (1982). Diurnal changes in compound eye fine structure in the blue crab *Callinectes*. *J. Ultrastruct. Res.* **78**, 40-59.
Van Gool, E. and Ringelberg, J. (2002). Relationship between fish kairomone concentration in a lake and phototactic swimming by *Daphnia*. *J. Plankton Res.* **24**, 713-721.
Warrant, E. J. (1999). Seeing better at night: life style, eye design and the optimum strategy of spatial and temporal summation. *Vision Res.* **39**, 1611-1630.
Warrant, E. J. (2008). Seeing in the dark: vision and visual behaviour in nocturnal bees and wasps. *J. Exp. Biol.* **211**, 1737-1746.
Warrant, B. E., Oskarsson, M. and Malm, H. (2014). The remarkable visual abilities of nocturnal insects: neural Principles and bioinspired night-vision algorithms. *Proc. IEEE.* **102**, 1411-1426.
Welch, J. and Forward, R. (2001). Flood tide transport of blue crab, *Callinectes sapidus*, postlarvae: behavioral responses to salinity and turbulence. *Mar. Biol.* **139**, 911-918.
Williamson, C. E., Fischer, J. M., Bollens, S. M., Overholt, E. P. and Breckenridge, J. K. (2011). Toward a more comprehensive theory of zooplankton diel vertical migration: integrating ultraviolet radiation and water transparency into the biotic paradigm. *Limnol. Oceanogr.* **56**, 1603-1623.
Yang, X. L., Zheng, W. Y., Chai, M. J. and Zhang, L. (1986). Circadian rhythms of the ERG of the crab *Scylla serrata*. *Acta Zool. Sinica* **32**, 122-129.
Yuan, W. J., Wang, Q. and Hu, X. Y. (1997). Ultrastructure changes of the photoreceptor in the crab *Eriocheir sinensis* by diurnal photoperiodism. *Acta Zool. Sinica* **43**, 344-352.